Downregulation of *PKD1* by shRNA Results in Defective Osteogenic Differentiation via cAMP/PKA Pathway in Human MG-63 Cells

Ni Qiu,[1,2] Honghao Zhou,[1] and Zhousheng Xiao[2]*

[1]*Institute of Clinical Pharmacology, Central South University, Changsha, Hunan, 410078, China*
[2]*Division of Nephrology, Department of Medicine, University of Tennessee Health Science Center, Memphis, TN 38165,*

ABSTRACT

Mutations and/or deletions of *Pkd1* in mouse models resulted in attenuation of osteoblast function and defective bone formation; however, the function of PKD1 in human osteoblast and bone remains uncertain. In the current study, we used lentivirus-mediated shRNA technology to stably knock down *PKD1* in the human osteoblastic MG-63 cell line and to investigate the role of PKD1 on human osteoblast function and molecular mechanisms. We found that a 53% reduction of *PKD1* by *PKD1* shRNA in stable, transfected MG-63 cells resulted in increased cell proliferation and impaired osteoblastic differentiation as reflected by increased BrdU incorporation, decreased alkaline phosphatase activity, and calcium deposition and by decreased expression of *RUNX2* and *OSTERIX* compared to control shRNA MG-63 cells. In addition, knockdown of *PKD1* mRNA caused enhanced adipogenesis in stable *PKD1* shRNA MG-63 cells as evidenced by elevated lipid accumulation and increased expression of adipocyte-related markers such as *PPARγ* and *aP2*. The stable *PKD1* shRNA MG-63 cells exhibited lower basal intracellular calcium, which led to attenuated cytosolic calcium signaling in response to fluid flow shear stress, as well as increased intracellular cAMP messages in response to forskolin (10 μM) stimulation. Moreover, increased cell proliferation, inhibited osteoblastic differentiation, and osteogenic and adipogenic gene markers were significantly reversed in stable *PKD1* shRNA MG-63 cells when treated with H89 (1 μM), an inhibitor of PKA. These findings suggest that downregulation of *PKD1* in human MG-63 cells resulted in defective osteoblast function via intracellular calcium-cAMP/PKA signaling pathway. J. Cell. Biochem. 113: 967–976, 2012. © 2011 Wiley Periodicals, Inc.

KEY WORDS: *PKD1*; shRNA KNOCKDOWN; OSTEOGENIC DIFFERENTIATION; cAMP/PKA PATHWAY: MG-63

U
sing mouse genetic approaches in vivo and primary osteoblast cultures in vitro, we recently identified an essential role of polycystin-1(PC1), the product of the *Pkd1* gene, in mouse osteoblast and bone development [Xiao et al., 2006, 2008, 2010], as well as postnatal bone homeostasis and bone mechanosensing [Xiao et al., 2011]. We found that *Pkd1* mRNA was highly expressed in osteoblastic lineage and played an important role in both skeletal development and postnatal bone homeostasis through intracellular calcium and Runx2-dependent signaling mechanisms [Xiao et al., 2006, 2008, 2010]. More recently, we demonstrated that *Pkd1* null osteoblasts markedly lost their intracellular calcium response to fluid shear stress in vitro and that conditional deletion of *Pkd1* from osteocytes resulted in osteopenia and a significant decrease in the anabolic response to mechanical loading in vivo [Xiao et al., 2011]. These findings suggest a role of intracellular calcium in PC1-mediated osteoblast function in bone, similar to

renal epithelial cells [Al-Bhalal and Akhtar, 2005; Yoder et al., 2006]. However, how closely these studies in mice reflect human physiology and pathophysiology remains uncertain, because patients with autosomal dominant polycystic kidney disease (ADPKD) do not have clinically apparent skeletal abnormalities [Boucher and Sandford, 2004; Wilson, 2004; Harris and Torres, 2009].

It has been demonstrated that vascular smooth muscle and cystic epithelial cells from human and mouse ADPKD kidney exhibit lower basal intracellular calcium but higher intracellular cAMP content [Yamaguchi et al., 2000; Marfella-Scivittaro et al., 2002; Gattone et al., 2003; Qian et al., 2003; Yamaguchi et al., 2004; Kip et al., 2005; Starremans et al., 2008]. In cystic epithelial cells from human ADPKD kidney, there is a cAMP-induced cell-growth switch characterized by cAMP-mediated inhibition of proliferation in normal renal epithelial cells and cAMP-induced cell growth in cystic

epithelial cells [Yamaguchi et al., 2004, 2006; Wallace, 2011]. These data suggest that abnormal cAMP/PKA signaling plays an important role in the pathophysiology of ADPKD kidneys. In human and mouse models, inappropriate activation of the cAMP signaling pathway leads to the development of bone diseases, such as defects in intramembranous ossification and osteochondrodysplasia [Jones et al., 2010; Tsang et al., 2010]. In addition, there is evidence showing that parathyroid hormone (PTH) and other drugs such as forskolin increased the level of intracellular cAMP/PKA signaling and inhibited osteoblastic differentiation [Koh et al., 1999]. Moreover, cAMP/PKA pathway facilitated the degradation of Runx2 bone-specific transcription factor through the ubiquitin/proteasome-dependent mechanism [Tintut et al., 1999].

In the current study, to determine whether PKD1 has an important role in human osteoblasts, we used lentivirus-mediated shRNA technology to stably silence *PKD1* mRNA messages and examine the effects of PKD1 on osteoblast function and intracellular signals in the human osteoblastic MG-63 cell line. We demonstrated that stable, knocked down *PKD1* resulted in increased cell proliferation, attenuated osteogenic differentiation, and enhanced adipogenesis associated with impairment of intracellular calcium and enhancement of cAMP/PKA signaling in human MG-63 osteoblasts. These results indicate that PKD1 has a direct role in regulating human osteoblast commitment and function.

MATERIALS AND METHODS

CELL CULTURE

Human osteoblast-like cells (MG-63) were obtained from the American Type Culture Collection (ATCC, Manassas, VA). MG-63 cells were cultured in EMEM (Eagle's minimum essential medium, ATCC) containing 5% heat-inactivated fetal bovine serum (FBS) (HyClone, Lakewood, NJ) and 1% penicillin and streptomycin (P/S) (Sigma–Aldrich, St. Louis, MO) at 37°C in 5% CO_2 humidified air. The MG-63 cells stably expressing *PKD1* shRNA were maintained in growth medium with G418 ($300 \mu g/ml$). For osteogenic differentiation, the cells were plated at $3 \times 10^3/cm^2$ to six-well plates and grown in osteogenic differentiation medium (EMEM with 0.1% FBS, 1% P/S, 5 mM β-glycerophosphate, $25 \mu g/ml$ L-ascorbic acid, and $10 \eta M$ 1,25-dihydroxyvitamin D_3) [Franceschi and Young, 1990]. For adipogenic differentiation, cells were grown in adipogenic differentiation medium (EMEM with 0.1% FBS, 1% P/S, supplemented with $0.5 \mu M$ 3-isobutyl-1-methylxantine, $1 \mu M$ dexamethasome, and $10 \mu g/ml$ insulin) for 21 days [Janderova et al., 2003].

shRNA EXPRESSION VECTOR CONSTRUCTION AND TRANSFECTION

The three highest scoring shRNA sequences targeted for human *PKD1* were chosen by Genscript's siRNA design tool: *PKD1* siRNA1, 5′-TCC TGA CCG TGC TGG CAT CTA-3′; *PKD1* siRNA2, 5′-CGT GGT CTT CAA TGT CAT TTA-3′; and *PKD1* siRNA3, 5′-CAA CAA GAT TTC TAC GTT AGA-3′. The shRNA negative control (5′-TAC ATC ATA GCA GGT ATA TCA-3′) was obtained from GenScript USA Inc. (Piscataway, NJ), which has no homology to any human mRNA sequence in the NCBI Reference Sequence (RefSeq) Database. pRNAT-U6.2/Lenti™ was purchased (GenScript USA Inc.) as the
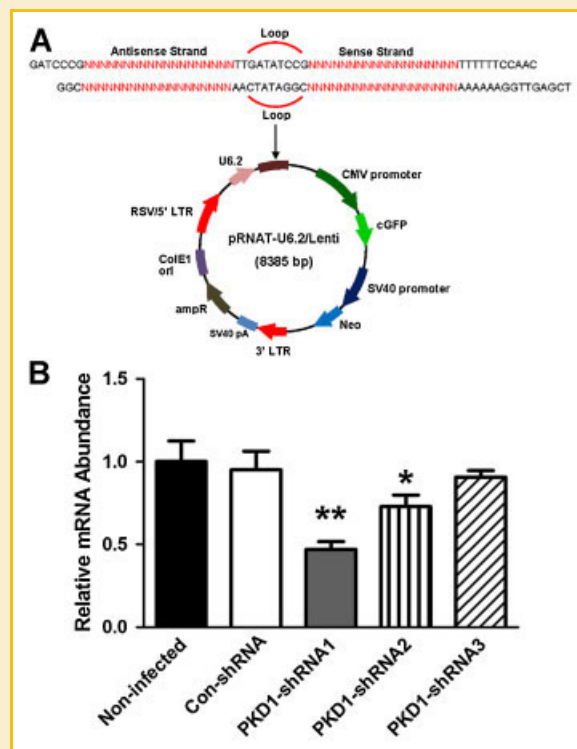

Fig. 1. Knockdown efficiency of lentivirus-mediated *PKD1* shRNA in stable transfected human MG-63 cells. A: The diagram of the lentivirus-mediated *PKD1* shRNA expression vector. *PKD1* shRNA sequences were inserted downstream of the U6 promoter in pRNAT-U6/Lenti. The red sequence is equivalent to the *PKD1* mRNA target sequence as described in Materials and Methods section. U6.2, modified Pol III promoter; shRNA, small hairpin RNA; *CMV*, CMV promoter; cGFP, coral green fluorescent protein. B: Quantitative real-time RT–PCR analysis of total *PKD1* transcripts from stable, transfected human MG-63 cells. *PKD1* mRNA expression was normalized by housekeeping gene β-*ACTIN*. Data are expressed as the mean ± SD from four individual samples. *, **Significant difference from control shRNA MG-63 cells at $P < 0.05$, $P < 0.01$, respectively. [Color figure can be seen in the online version of this article, available at http://wileyonlinelibrary.com/journal/jcb]

targeting shRNA expression vector (Fig. 1A). Two chemically synthesized DNA oligonucleotides that encode the *PKD1* shRNA sequence were designed and annealed for insertion into the vector. For *PKD1* siRNA1, sense cassette: 5′-GAT CCC GTA GAT GCC AGC ACG GTC AGG ATT GAT ATC GT CCT GAC CGT GCT GGC ATC TAT TTT TTC CAA C-3′; antisense cassette: 5′-TCG AGT TGG AAA AAA TAG ATG CCA GCA CGG TCA GGA CGG ATA TCA ATC CTG ACC GTG CTG GCA TCT ACG G-3′. For *PKD1* siRNA2, sense cassette: 5′-GAT CCC GTA AAT GAC ATT GAA GAC CAC GTT GAT ATC CGC GTG GTC TTC AAT GTC ATT TAT TTT TTC CAA C-3′; antisense cassette: 5′-TCG AGT TGG AAA AAA TAA ATG ACA TTG AAG ACC ACG CGG ATA TCA ACG TGG TCT TCA ATG TCA TTT ACG G-3′ For *PKD1* siRNA3, sense cassette: 5′GAT CCC GTC TAA CGT AGA AAT CTT GTT GTT GAT ATC CGC AAC AAG ATT TCT ACG TTA GAT TTT TTC CAA C-3′ antisense cassette: 5′-TCG AGT TGG AAA AAA TAA ATG ACA TTG AAG ACC ACG CGG ATA TCA ACG TGG TCT TCA ATG TCA TTT ACG G-3′. For control shRNA sequence, sense cassette: 5′-GAT CCC ATG ATA TAC CTG CTA TGA TGT TTG ATA TCC GAC ATC ATA GCA GGT ATA TCA TTT TTT CCA AC-3′;

antisense cassette: 5′-TCG AGT TGG AAA AAA ATG ATA TAC CTG CTA TGA TGT CGG ATA TCA AAC ATC ATA GCA GGT ATA TCA TGG-3′. The resulting double-stranded DNA (dsDNA) oligo was inserted into the BamH I and XhoI sites of the pRNAT-U6.2/Lenti to generate *PKD1* shRNA1, shRNA2, shRNA3, or control shRNA expression vector. The accuracy of the inserted into the recombinants was verified by restriction enzyme analysis and sequencing. We used ViraPower™ Lentiviral Expression System (Invitrogen Corporation, Carlsbad, CA, USA) to generate lentivirus supernants from HEK293FT cells. In brief, HEK293FT cells were seeded in 10-cm dishes at 5×10^6 cells/dish. After cells reached 90–95% confluence, the constructed shRNA expression vector (3 μg/dish) and ViraPower™ Packaging Mix (9 μg/dish) with Lipofectamine™ 2000 (Invitrogen Corporation) were transfected into HEK293FT cells. Twelve hours after initiating transfection, the plasmid–lipofectamine solution was removed, and the cell growth medium without antibiotics was added. The lentivirus-containing supernatants were harvested 48 and 72 h posttransfection. The MG-63 cells were plated at 30–50% confluence and transfected with appropriate dilutions of lentivirus supernatants. Forty-eight hours after transfection, the cells were cultured in cell growth medium containing G418 (300 μg/ml) to obtain the stable, transfected MG-63 cells. After several selection, colonies (>200) were pooled to minimize effects secondary to variable integration sites.

IMMUNOFLUORESCENCE

MG-63 cells were grown on collagen-coated 4-well chambers at 1×10^5 cells/well and kept at confluence for at least 3 days. At the end of the culture, the cells were washed three times with PBS, fixed with cold 4% paraformaldehyde/0.2% Triton for 10 min at room temperature, and washed with PBS three times. The cells were incubated for 30 min in 1% BSA before incubation with the primary acetylated alpha-tubulin antibody (1:4000, T6793, Sigma–Aldrich) for 1 h at room temperature. After washing three times in PBS, cells were treated with secondary Texas Red-labeled anti-mouse IgG (715-076-150, Jackson ImmunoResearch, West Grove, PA) in 1% BSA for 1 h at room temperature and washed three times in PBS before being mounted with ProLong® Gold antifade reagent (P36935, Invitrogen Corporation) that contained diamidino-2-phenylindole (DAPI blue) as a nuclear counterstain for all nuclei. Photographs were taken under a microscope with magnifications of 40x for counting the number of primary cilia and 100x for measuring the length of primary cilia in cultured MG-63 cells as previously described [Qiu et al., 2010].

REAL–TIME REVERSE TRANSCRIPTASE POLYMERASE CHAIN REACTION

Stable transfected MG-63 cells were cultured in different medium for the indicated time points. Total RNA was extracted by TRIzol Reagent (Invitrogen Corporation) and subsequently purified using RNeasy Mini Kit (Qiagen, Valencia, CA). Total RNA (1 μg) was used to synthesize cDNA by using the iScript cDNA synthesis kit (Bio-Rad, Hercules, CA). Quantitative real-time polymerase chain reaction (PCR) was performed using SsoFast EvaGreen Supermix on a CFX96 Touch™ Real-Time PCR system (Bio-Rad) in 10 μl final volume (comprising $1 \times$ SsoFast EvaGreen supermix, 0.2 μM forward and reverse primers, and 20 ηg of cDNA). Post-PCR melting curves confirmed the specificity of single-target amplification, and fold changes in gene expressions were normalized to housekeeping gene β-*ACTIN*. Gene-specific primers sets are shown in the Table I.

PROLIFERATION ASSAY

Cell proliferation was detected by bromodeoxyuridine (BrdU) incorporation assays as described by the manufacturer (QIA58, Calbiochem, Gibbstown, NJ). The cells were seeded into 96-well plates at a density of 1×10^4/well in growth medium for 24 h and then serum starved for 12 h. Then cells were switched to fresh medium containing BrdU for the indicated time points.

Ca^{2+} INFLUX ANALYSIS

The basal intracellular calcium ($[Ca^{2+}]_i$) concentration and flow-induced intracellular calcium response were measured in stable, transfected MG-63 cells as previously described [Xiao et al., 2011]. In brief, the MG-63 cells were cultured on type I rat tail collagen-coated 40-mm diameter glass slides at 80–90% confluence in EMEM containing 2% FBS and 1% P/S for 3 days. Then the cells were incubated with 3 μM of Fure-2/AM (Invitrogen Corporation), a Ca^{2+}-responsive fluorescent dye, for 30 min at 37°C and then switched to fresh Hank's Balanced Salt Solution (HBSS) for another 30 min prior to experiments. The flow media consisted of HBSS that contained 2% FBS and 20 mM HEPES. A glass slide was then placed in an FCS2 parallel plate flow chamber (Bioptechs, Inc., Butler, PA), $0.25 \times 14 \times 22$ mm^3. A fresh bolus of flow media was added to the chamber, and the cells were left undisturbed for 30 min. The chamber was mounted on the stage of an inverted microscope with CCD camera to allow real-time record of fluorescence intensity (F340/F380 ratio) to generate ratiometric video images of individual static cells or cells exposed to pulsatile laminar fluid flow (Intracellular Imaging, Inc., Cincinnati, OH).

TABLE I. Primer sequences used in real-time RT-PCR

Gene	Accession no.	Forward primer	Reverse primer
PKD1	NM_000296	5′-TCCGTACAACGAGTCCTTCC-3′	5′-AAGGCATTAGATCCAGCAC-3′
RUNX2	NM_004348	5′-CAGACCAGCAGCACTCCATA-3′	5′-CAGCGTCAACACCATCATTC-3′
OSTERIX	NM_152860	5′-GCCAGAAGCTGTGAAACCTC-3′	5′-GCTGCAAGCTCTCCATAACC-3′
PPARγ	NM_015869	5′-GCCGAGAAGGAGAAGC-3′	5′-TGGTCAGCGGGAAGG-3′
aP2	NM_001442	5′-ATGGGATGGAAAATCAACCA-3′	5′-GTGGAAGTGACGCCTTTCAT-3′
GLI2	NM_005270	5′-ACGGCTGACATTCGGCTAAC-3′	5′-CCTTTGAAAGGTTTTGGCCAA-3′
BMP2	NM_001200	5′-TCAAGCCAAACACAAACAGC-3′	5′-ACGTCTGAACAATGGCATGA-3′
β-*ACTIN*	NM_001101	5′-CGGCATCGTCACCAACTG-3′	5′-GGCACACGCAGCTCATTG-3′

ASSAY OF INTRACELLULAR cAMP

The intracellular cAMP level was determined using a cAMP enzyme immunoassay system (GE Healthcare, Pittsburgh, PA). Stable, transfected MG-63 cells were seeded at a density of 1×10^4/well in 96-well plates (n = 5) overnight; the medium was replaced with fresh medium without FBS for 12 h. The cells were switched to fresh medium (containing 1% FBS) with forskolin (10 μM) or vehicle medium control (DMSO) for 30 min. Then the medium was removed, and the cAMP level in the cultured cells was determined according to the manufacturer's instructions.

NUCLEOFECTION AND DUAL LUCIFERASE REPORTER ASSAY

To evaluate the cAMP-directed gene transactivation in stable, transfected *PKD1* or control shRNA MG-63 cells, the pCRE-luciferase (pCRE-luc) reporter construct (Stratagene, La Jolla, CA), a cAMP-inducible luciferase-expressing plasmid, was used in the following nucleofection experiment. In brief, MG-63 cells were grown to a confluence of 70–80%. After trypsinization, a number of 2×10^6 cells were transfected with 3.0 μg of pCRE-luc, 3.0 μg of pcDNA3.1 empty vector, and 0.6 μg of *Renilla* luciferase-null (RL-null) as internal control plasmid by electroporation by using Cell Line Nucleofector Kit R according to the manufacturer's protocol (Amaxa, Inc., Gaithersburg, MD). The cells were cultured in the fresh growth medium without antibiotics overnight; the medium was replaced with fresh medium without FBS for 12 h. Then the cells were switched to fresh medium containing 1% FBS with forskolin (10 μM) or vehicle (DMSO) control for 24 h. The cells were harvested, and luminescence from both the firefly and Renilla reporters was determined with the Dual-Luciferase Reporter Assay System (Promega, Madison, WI) according to the manufacturer's instructions. The GloMax® 20/20 Luminometer (Promega) was used to measure the luminescence activity. Relative luminescence units (RLU) are defined as the ratio between firefly and Renilla luciferase. All nucleofections were performed in triplicate.

ALKALINE PHOSPHATASE (ALP) ACTIVITY MEASUREMENT

Alkaline phosphatase activity was detected in the cell lysates by enzymatic colorimetric method as previous described [Xiao et al., 2004]. Briefly, cell layers were rinsed three times with PBS and then scraped into sterile water followed by sonication and centrifugation to remove cellular debris. Llysate supernant (100 μl) was then mixed with 400 μl diethanolamine (1.5 M, pH 10.3) and 100 μl of the freshly prepared colorimetric substrate *para*-nitrophenyl phosphate (90 mM), and incubated at 37°C for 30 min. The enzymatic reaction was stopped by adding 2.4 ml of 0.1 N NaOH solution. The optical density of the yellow product *para*-nitrophenol was determined spectrophotometrically at 405 ηm. The DNA content of the cell lysates was measured with picogreen dsDNA quantitation kit (Invitrogen Corporation), and ALP activity was then expressed as *para*-nitrophenol produced in ηmol/min/μg of DNA.

ALIZARIN RED S STAINING

Alizarin Red S staining was performed to detect matrix mineralization. The osteogenic cell cultures were rinsed three times with PBS followed by fixation in ice-cold 70% ethanol for 1 h, then stained with 40 mM Alizarin Red S (Sigma–Aldrich), pH 4.2, for 10 min at room temperature. To quantify the calcium content, the stained cultures underwent a distaining procedure that used 10% cetylpyridinium chloride in 10 mM sodium phosphate, pH 7.0, for 15 min at room temperature. The eluted Alizarin Red S concentration was determined by absorbance measurement at 562 nm, and protein concentration of the cell lysates was measured with a Pierce® BCA Protein Assay Kit (Pierce Biotechnology, Rockford, IL).

OIL–RED O STAINING

To detect lipid accumulation, Oil-Red O staining was performed with 5 mM Oil-Red O solution (Sigma–Aldrich). The adipogenic cultures were fixed in 10% formalin for at least 1 h and stained with fresh Oil Red-O working solution for 5 min. After staining, the cultures were rinsed with tap water at room temperature until the water rinsed off clear and eluted by 100% isopropanol for 10 min at room temperature. Aliquots of Oil-Red O were measured at 500 nM.

STATISTICAL ANALYSIS

We evaluated differences between two groups by unpaired *t*-test and multiple groups by one-way analysis of variance. All values are expressed as means ± SD. All computations were performed using the GraphPad Prism5 (GraphPad Software, Inc., La Jolla, CA).

RESULTS

LENTIVIRUS–MEDIATED shRNA KNOCKDOWN OF *PKD1* mRNA IN MG–63 CELLS

Three *PKD1* shRNAs constructs were delivered into human MG-63 cells by means of pRNAT-U6.2/Lenti™ (Fig. 1A), a lentiviral vector containing a human U6 promoter to drive the expression of the shRNA. The relative abundance of *PKD1* mRNA in stable, transfected control shRNA and *PKD1* shRNA MG-63 cells was analyzed by quantitative real-time RT-PCR. Compared to non-transfected MG-63 cells, there was no difference of *PKD1* mRNA expression in stable, transfected control shRNA MG-63 cells. However, three stable, transfected *PKD1* shRNA MG-63 cells exhibited a range from 10% to 60% suppression of *PKD1* mRNA expression (Fig. 1B). In the following experiments, we chose to use stable, transfected *PKD1* shRNA1 MG-63 cells (a 53% reduction of *PKD1* mRNA by shRNA1) for further cellular function and signaling pathway analysis.

shRNA KNOCKDOWN OF *PKD1* mRNA ON CELL PROLIFERATION, OSTEOBLASTIC DIFFERENTIATION AND MATURATION, AND ADIPOGENESIS IN MG–63 CELLS

To determine the role of PKD1 on human osteoblast function ex vivo, we used stable, transfected *PKD1* shRNA MG-63 cells to examine cell proliferation, osteoblastic differentiation, and gene expression profiles in osteogenic conditions. Consistent with our previous report [Xiao et al., 2010; Xiao and Quarles, 2010], shRNA knockdown of *PKD1* mRNA resulted in a significant increase of cell proliferation, evidenced by a higher BrdU incorporation compared to the control shRNA MG-63 cells (Fig. 2A). The shRNA knockdown of *PKD1* mRNA in MG-63 cells also impaired osteoblastic differentiation. As shown in Fig. 2B and C, the MG-63 cells showed a time-dependent increase of ALP activity and calcium deposition
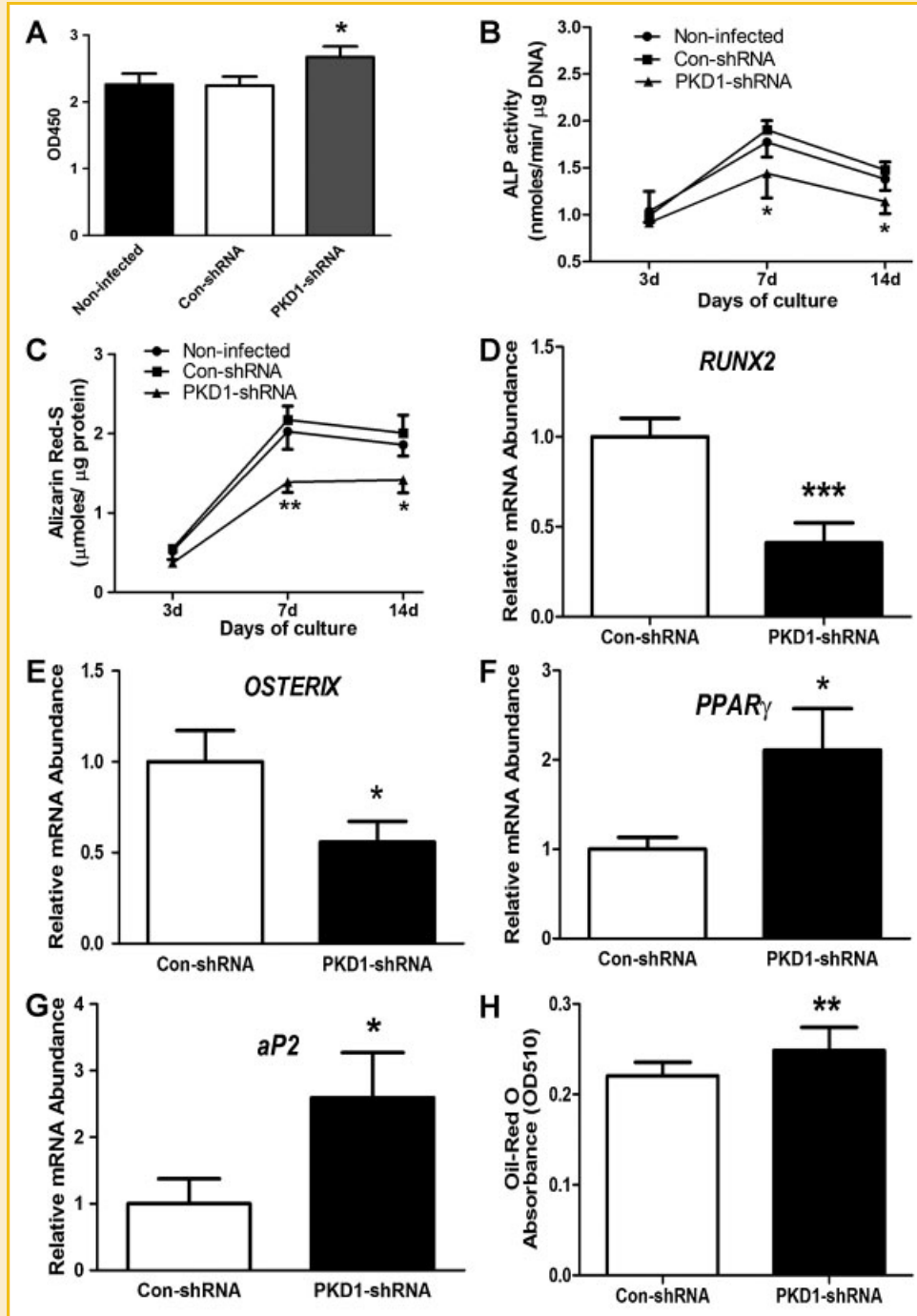
Fig. 2. shRNA knockdown of *PKD1* mRNA on proliferation, osteoblastic differentiation, and adipogenesis in human MG-63 cells. A: BrdU incorporation for 6 h. B: ALP activity during 14 days of osteogenic culture. C: Quantification of mineralization. D–G: Osteogenic and adipogenic gene expression profiles by quantitative real–time RT–PCR at day 7. H: Relative Oil Red O absorbance from 21 days of adipogenic cultures. Data are expressed as the mean ± SD from three independent experiments. *, **, ***Significant difference from control shRNA MG-63 cells at $P < 0.05$, $P < 0.01$, and $P < 0.001$, respectively.

up to 14 days of osteogenic culture, but the *PKD1* shRNA MG-63 cells had time-dependent lower ALP activity (Fig. 2B), diminished calcium deposition in extracellular matrix (Fig. 2C), and reduced osteoblastic differentiation markers, including *RUNX2* and *OSTERIX* (Fig. 2D and E) compared to control shRNA MG-63 cells. In contrast, we found that the expression of adipocyte marker

genes, *PPARγ* and *aP2*, were significantly increased in the *PKD1* shRNA MG-63 cells compared with control shRNA MG-63 cells (Fig. 2F and G). In addition, the *PKD1* shRNA MG-63 cells exhibited increased lipid accumulation and Oil-Red O staining in adipogenic medium (Fig. 2H), indicating that shRNA knockdown of *PKD1* mRNA in human osteoblasts promoted adipogenesis. These findings

suggest an impairment of osteogenesis and enhancement of adipogenesis in the *PKD1* shRNA MG-63 cell cultures.

CHANGES OF PRIMARY CILIA, INTRACELLULAR CALCIUM, AND CAMP SIGNALING IN STABLE *PKD1* SHRNA TRANSFECTED MG–63 CELLS

Forskolin increased cilia length in control shRNA MG-63 cells, and shRNA knockdown of *PKD1* also increased cilia length. However, PKA inhibitor H89 (1.0 μM) blocked *PKD1* shRNA-induced cilia length increase (Fig. 3A and B), indicating that the cAMP/PKA pathway is involved in primary cilia formation in human osteoblasts. However, there were no obvious number differences in the primary cilia among these four groups (data not shown). Compared with control shRNA MG-63 cells, we found that *PKD1* shRNA MG-63 cells had a significantly lower basal intracellular calcium level (Fig. 3C). To investigate whether PKD1 had a role in flow-induced intracellular calcium response, the MG-63 cells were exposed to 6.24 dynes/cm^2 pulsatile laminar fluid flow. On fluid stimulation, we detected an immediate rise in intracellular calcium throughout the control shRNA MG-63 cell population and a peak roughly 10–20 s after stimulation (Fig. 3D). The [Ca^{2+}]$_i$ levels then rapidly decreased but were maintained at moderate levels for 50–60 s before returning to baseline. In contrast, when we exposed *PKD1* shRNA MG-63 cells to an identical flow stimulus, we detected a marked reduction in intracellular calcium response curve (Fig. 3D). However, 10 mM caffeine still resulted in normal calcium influx in *PKD1* shRNA MG-63 cells after flow stimulus (data not shown), indicating the viability of *PKD1* shRNA MG-63 cells in the loading chamber. Our data suggest that the flow-induced [Ca^{2+}]$_i$ response requires polycystin complex in human osteoblasts and silencing of *PKD1* to attenuate fluid flow sensing in human osteoblasts.

To explore whether PKD1 plays a role in intracellular cAMP accumulation, we measured the changes of cAMP signaling by using a cAMP enzyme immunoassay system and pCRE-luciferase reporter construct in the absence or presence of forskolin (10 μM) stimulation. We found that both basal and forskolin-induced intracellular cAMP levels were higher in *PKD1* shRNA MG-63 cells than in control shRNA MG-63 cells (Fig. 3E). Similarly, the pCRE-luciferase activity was also significantly increased in *PKD1* shRNA MG-63 cells relative to control shRNA MG-63 cells (Fig. 3F). These results indicate that shRNA knockdown of *PKD1* mRNA in human osteoblasts promotes intracellular cAMP accumulation, a finding consistent with previous reports in human ADPKD renal epithelia cells [Yamaguchi et al., 2004, 2006].

THE EFFECT OF PKA INHIBITOR ON PKD1 shRNA MEDIATED ABNORMAL OSTEOBLAST FUNCTION IN MG–63 CELLS

To further establish the role of cAMP/PKA pathway in regulating osteoblast function in *PKD1* shRNA MG-63 cells, we examined the effects of PKA inhibitor (H89, a special antagonist for PKA) on cell proliferation, osteoblastic differentiation, and gene expression profiles. We found that BrdU incorporation was totally reversed in *PKD1* shRNA MG-63 cells after being treated with H89 (1.0 μM) for 6 h (Fig. 4A). Decreased ALP activity was partly restored in *PKD1* shRNA MG-63 cells after treatment with H89 (1.0 μM) for 7 days

(Fig. 4B). A quantitative real-time RT-PCR analysis revealed that *RUNX2*, an osteogenic marker, was markedly increased, while *aP2*, an adipogenic marker, was significantly decreased in *PKD1* shRNA MG-63 cells after being treated with H89 (1.0 μM) in osteogenic medium for 3 days (Fig. 4C and D). In addition, we observed that the inhibition of *GLI2* and *BMP2* expression by PKA activation was also rescued in *PKD1* shRNA MG-63 cells after being treated with PKA inhibitor H89 (1.0 μM) (Fig. 4E and F). As we know that PKA is the downstream target of cAMP signaling, these data suggest that PKD1 regulates osteoblast functions via cAMP/PKA pathway in human MG-63 cells.

DISCUSSION

In the current study, we used lentivirus-mediated shRNA technology to establish a stable, transfected *PKD1* shRNA MG-63 cell line that constantly knockdown *PKD1* mRNA in human osteoblast-like cells. We found that a 53% reduction of *PKD1* by shRNA in human MG-63 cells resulted in increased primary cilia length, cell proliferation, impaired osteogenic differentiation, and enhanced adipogenesis. Stable, transfected *PKD1* shRNA MG-63 cells had lower basal intracellular calcium that caused attenuated cytosolic calcium signaling in response to fluid flow shear stress and increased intracellular cAMP signaling in response to forskolin (10 μM) stimulation. Moreover, cell proliferation, osteogenic differentiation, osteogenic and adipogenic gene markers, and the length of primary cilia were restored when treated with PKA inhibitor (H89, 1 μM), which abolished cAMP-mediated downstream signal transduction. These findings suggest that PKD1 plays an important role in regulating human osteoblast function via the intracellular calcium-cAMP/PKA signaling pathway.

There is increasing evidence showing a role of intracellular calcium in polycystin complex-mediated cell signaling and function [Qian et al., 2003; Nauli et al., 2006; Yamaguchi et al., 2006; Casuscelli et al., 2009; Xiao et al., 2011]. In renal epithelial cells, PKD1 interacted with PKD2 to form a calcium channel, and mutations/deletions of *PKD1* and/or *PKD2* resulted in defective intracellular calcium signaling in response to fluid flow stimulation [Chen et al., 1999; Qian et al., 2003; Nauli et al., 2006; Yamaguchi et al., 2006]. We found that shRNA knockdown of *PKD1* mRNA displayed lower basal intracellular calcium and much less calcium influx in response to fluid flow-mediated mechanical stimulation. This finding is in agreement with our previous report in mouse *Pkd1* null osteoblasts [Xiao et al., 2011]. Calcium has been recognized as a critical mediator for osteoblasts and osteocytes to respond to its environmental cues such as hormone, cytokine, and mechanical stimulation [Xia and Ferrier, 1992; Bikle and Halloran, 1999; Henriksen et al., 2006; Kamioka et al., 2006]. Increase of calcium influx in bone cells (e.g., during exercise) leads to increased bone formation and resorption, whereas loss of calcium signaling (e.g., during spaceflight or from disuse) causes acute and severe bone loss [Bikle and Halloran, 1999]. Calcium signaling has also been proven to negatively regulate commitment to adipocyte differentiation by preventing the expression and transcriptional activation of critical proadipogenic transcription factors such as PPARγ and CCAAT
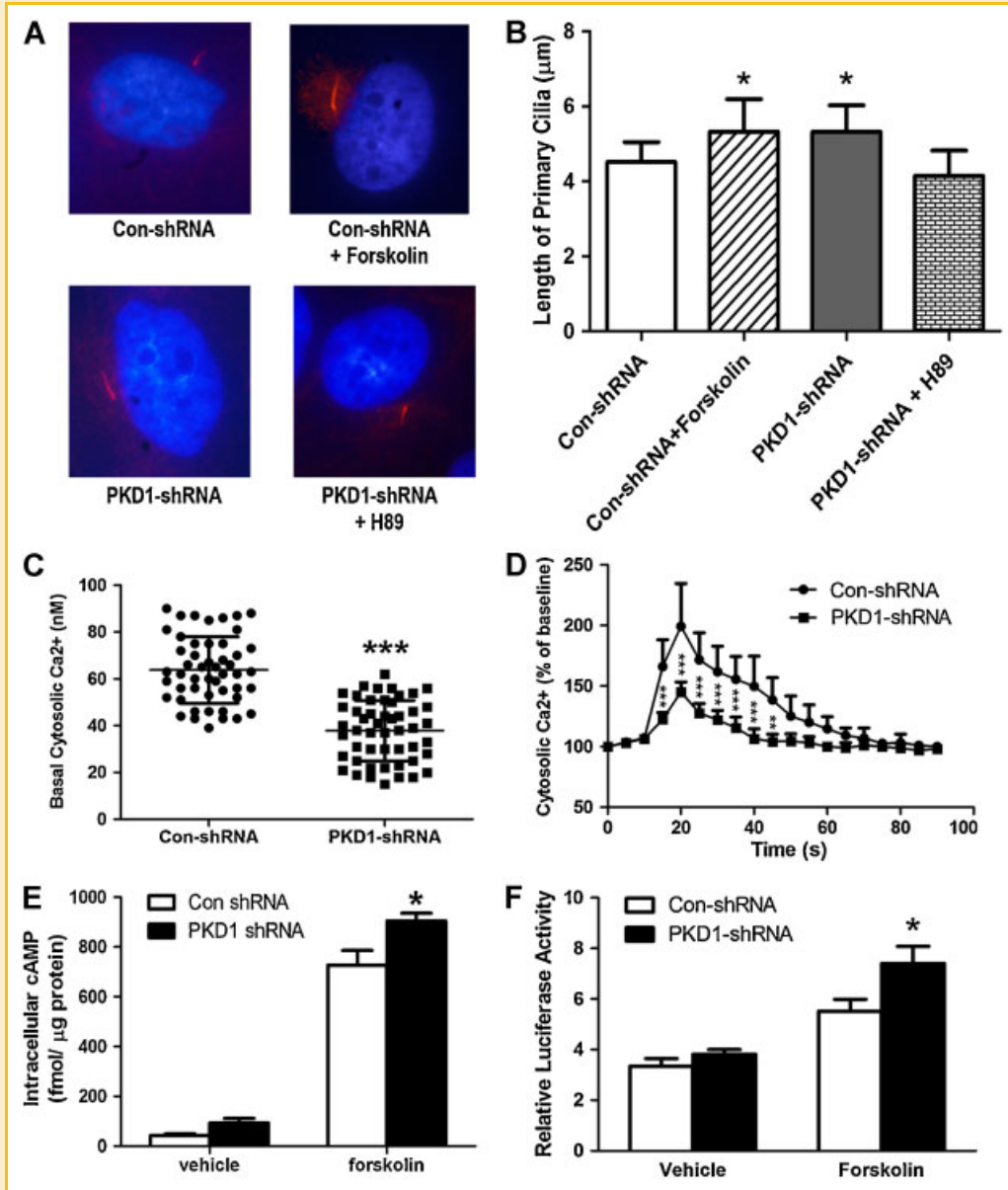
Fig. 3. shRNA knockdown of *PKD1* mRNA on intracellular calcium and cAMP signaling in MG-63 cells. A,B: Immunofluorescence of primary cilia in cultured MG-63 cells. Acetylated α-tubulin was used both as cilia marker (Red) and to measure cilia length as described in Materials and Methods section. Counterstaining with a nuclear marker (DAPI blue) was used to count the cell numbers. C: Basal intracellular calcium ($[Ca^{2+}]_i$) levels (n = 50). D: Fluid flow–induced $[Ca^{2+}]_i$ response curve (n = 4). A $[Ca^{2+}]_i$ response curve was recorded in MG-63 cells after being exposed to 6.24 dynes/cm^2 pulsatile laminar fluid. E: Assays of intracellular cAMP levels using a cAMP enzyme immunoassay system. F: Measurement of pCRE-luciferase activity by transient transfection. Data are mean ± SD from three independent experiments. *, **, ***Significant difference from control shRNA MG-63 cells at $P < 0.05$, $P < 0.01$, and $P < 0.001$, respectively. [Color figure can be seen in the online version of this article, available at http://wileyonlinelibrary.com/journal/jcb]

enhancer-binding protein α (C/EBPα) [Neal and Clipstone, 2002; Meldolesi, 2008; Szabo et al., 2008; Sun et al., 2011]. In agreement with our previous findings [Qiu et al., 2010; Xiao et al., 2010, 2011], shRNA knockdown of *PKD1* mRNA in human MG-63 cells resulted in impaired osteogenic differentiation and enhanced adipogenesis, indicating that polycystin complex plays an important role in regulating calcium signaling and cellular commitment during early stages of human osteoblast development.

The unique relationship between intracellular calcium and cAMP signaling has been established [Qian et al., 2003; Yamaguchi et al., 2004, 2006; Wallace, 2011]. In ADPKD cells, mutations of *PKD* genes lead to low intracellular calcium signaling; relieve Akt (a calcium-dependent kinase) inhibition of B-Raf; and allow cAMP stimulation of B-Raf, ERK, and cell proliferation [Wallace, 2011]. Similar to Wallace's report, stable, transfected *PKD1* shRNA MG-63 cells had higher basal and forskolin-induced intracellular cAMP
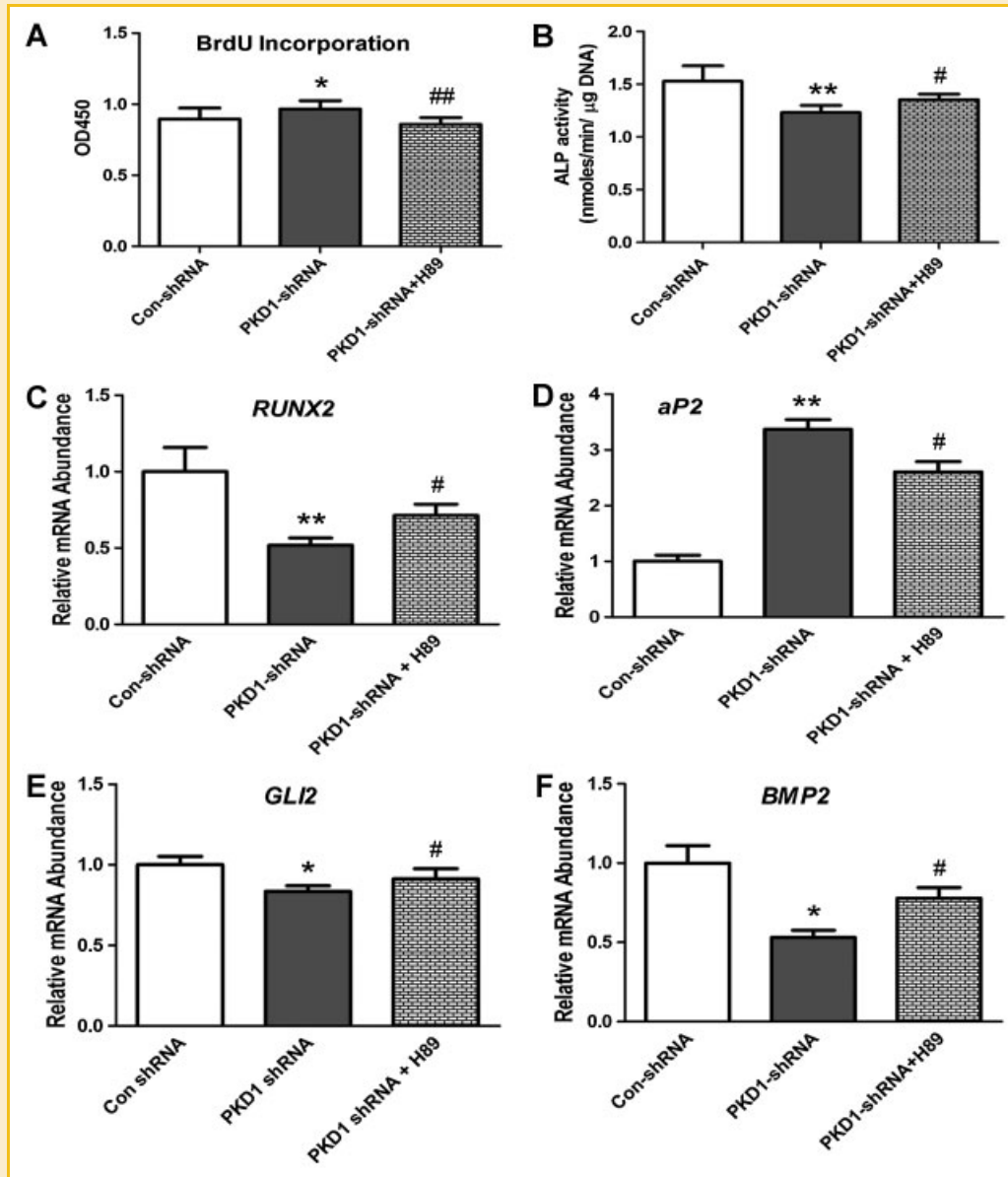
Fig. 4. The role of cAMP/PKA signaling on *PKD1* shRNA–mediated abnormal osteoblast function in MG-63 cells. A: BrdU incorporation for 6 h. B: ALP activity for 7 days. C,D: Expression of osteogenic and adipogenic markers by real–time RT–PCR. E,F: Transcriptional regulation of *GLI2* and *BMP2* expression by PKA inhibitor. *, **Significant difference from control shRNA MG-63 cells at $P < 0.05$ and $P < 0.01$, respectively. #, ##Significant difference from *PKD1* shRNA MG-63 cells at $P < 0.05$ and $P < 0.01$, respectively.

signaling, leading to an increase of cell proliferation, an inhibition of osteoblastic differentiation, and a stimulation of adipogenesis. Our findings are also consistent with the role of cAMP/PKA signaling in primary cilia and osteoblast function [Sutters et al., 2001; Tsuang et al., 2006; Nagata et al., 2009; Kwon et al., 2010]. It has been shown that intracellular cAMP and cAMP-dependent protein kinase regulate both cilia length and function in vascular endothelial cells [Abdul-Majeed et al., 2011]. According to previous reports, cilia length regulates intracellular calcium signaling in renal epithelial cells [Praetorius and Spring, 2001; Praetorius and Spring, 2003; Shiba et al., 2005] and the differentiated cells have longer cilia in response to extracellular environmental cues [Jackson, 2011; Saraga-Babic et al., 2011]. However, changes in cilia length are not always correlated to changes in cilia function [Abdul-Majeed et al., 2011]. In our studies, we did observe a significant increase of cilia length in stable, transfected *PKD1* shRNA MG-63 cells compared with control shRNA cells, but the flow-induced intracellular calcium response as well as osteoblastic differentiation were markedly decreased in the *PKD1* shRNA MG-63 cells because of less co-localization of polycystin complex to primary cilia by shRNA knockdown of *PKD1* [Nauli et al., 2003, 2006; Xiao et al., 2011]. In addition, increases of cAMP signaling by PTH fragments(1–34) and foskolin inhibited osteoblastic differentiation and mineralization in both MC3T3-E1 and rat primary calvarial cell cultures [Koh et al., 1999]. Activation of cAMP/PKA pathway by IBMX and forskolin also enhances adipogenesis and *PPARγ2* and *LPL* gene expressions,

but downregulates osteogenesis and the gene expression of *RUNX2* and *OSTEOPONTIN* in human primary mesenchymal stem cells [Yang et al., 2008]. Increase of cAMP/PKA activity also affected other critical osteogenic and adipogenic pathways in osteoblasts including Hh-Gli-BMP2 and MAPK/ERK signaling [Epstein et al., 1996; Wang et al., 2010]. It has been reported that PKA and GSK-3β (glycogen synthase kinase 3β) induced Gli protein phosphorylation, leading to proteolytic degradation of Gli protein proteolysis [Epstein et al., 1996], and disruption of Hh signaling causes metabolic bone diseases [Gao et al., 2001; Maeda et al., 2007]. The restoration of the Hh-Gli-BMP2 signaling by PKA inhibitor H89 in stable *PKD1* shRNA MG-63 cells suggests that the cAMP/PKA pathway plays an essential role in PKD1-regulated osteoblast function.

In summary, our findings suggest that PKD1 directly regulates human osteoblast commitment and function at least partially via intracellular calcium-cAMP/PKA signaling pathway. However, how cross-talk occurs between calcium signaling and cAMP/PKA pathway in *PKD1*-mediated osteoblast function remains to be elucidated.

REFERENCES

Abdul-Majeed S, Moloney BC, Nauli SM. 2011. Mechanisms regulating cilia growth and cilia function in endothelial cells. Cell Mol Life Sci DOI: 10.1007/s00018-011-0744-0.

Al-Bhalal L, Akhtar M. 2005. Molecular basis of autosomal dominant polycystic kidney disease. Adv Anat Pathol 12:126–133.

Bikle DD, Halloran BP. 1999. The response of bone to unloading. J Bone Miner Metab 17:233–244.

Boucher C, Sandford R. 2004. Autosomal dominant polycystic kidney disease (ADPKD, MIM 173900, PKD1 and PKD2 genes, protein products known as polycystin-1 and polycystin-2). Eur J Hum Genet 12:347–354.

Casuscelli J, Schmidt S, DeGray B, Petri ET, Celic A, Folta-Stogniew E, Ehrlich BE, Boggon TJ. 2009. Analysis of the cytoplasmic interaction between polycystin-1 and polycystin-2. Am J Physiol Renal Physiol 297:F1310–F1315.

Chen XZ, Vassilev PM, Basora N, Peng JB, Nomura H, Segal Y, Brown EM, Reeders ST, Hediger MA, Zhou J. 1999. Polycystin-L is a calcium-regulated cation channel permeable to calcium ions. Nature 401:383–386.

Epstein DJ, Marti E, Scott MP, McMahon AP. 1996. Antagonizing cAMP-dependent protein kinase A in the dorsal CNS activates a conserved Sonic hedgehog signaling pathway. Development 122:2885–2894.

Franceschi RT, Young J. 1990. Regulation of alkaline phosphatase by 1,25-dihydroxyvitamin D3 and ascorbic acid in bone-derived cells. J Bone Miner Res 5:1157–1167.

Gao B, Guo J, She C, Shu A, Yang M, Tan Z, Yang X, Guo S, Feng G, He L. 2001. Mutations in IHH, encoding Indian hedgehog, cause brachydactyly type A-1. Nat Genet 28:386–388.

Gattone VH II, Wang X, Harris PC, Torres VE. 2003. Inhibition of renal cystic disease development and progression by a vasopressin V2 receptor antagonist. Nat Med 9:1323–1326.

Harris PC, Torres VE. 2009. Polycystic kidney disease. Annu Rev Med 60: 321–337.

Henriksen Z, Hiken JF, Steinberg TH, Jorgensen NR. 2006. The predominant mechanism of intercellular calcium wave propagation changes during long-term culture of human osteoblast-like cells. Cell Calcium 39:435–444.

Jackson PK. 2011. Do cilia put brakes on the cell cycle? Nat Cell Biol 13:340–342.

Janderova L, McNeil M, Murrell AN, Mynatt RL, Smith SR. 2003. Human mesenchymal stem cells as an in vitro model for human adipogenesis. Obes Res 11:65–74.

Jones GN, Pringle DR, Yin Z, Carlton MM, Powell KA, Weinstein MB, Toribio RE, La Perle KM, Kirschner LS. 2010. Neural crest-specific loss of Prkar1a causes perinatal lethality resulting from defects in intramembranous ossification. Mol Endocrinol 24:1559–1568.

Kamioka H, Sugawara Y, Murshid SA, Ishihara Y, Honjo T, Takano-Yamamoto T. 2006. Fluid shear stress induces less calcium response in a single primary osteocyte than in a single osteoblast: Implication of different focal adhesion formation. J Bone Miner Res 21:1012–1021.

Kip SN, Hunter LW, Ren Q, Harris PC, Somlo S, Torres VE, Sieck GC, Qian Q. 2005. [Ca2+]i reduction increases cellular proliferation and apoptosis in vascular smooth muscle cells: Relevance to the ADPKD phenotype. Circ Res 96:873–880.

Koh AJ, Beecher CA, Rosol TJ, McCauley LK. 1999. 3′,5′-Cyclic adenosine monophosphate activation in osteoblastic cells: Effects on parathyroid hormone-1 receptors and osteoblastic differentiation in vitro. Endocrinology 140:3154–3162.

Kwon RY, Temiyasathit S, Tummala P, Quah CC, Jacobs CR. 2010. Primary cilium-dependent mechanosensing is mediated by adenylyl cyclase 6 and cyclic AMP in bone cells. FASEB J 24:2859–2868.

Maeda Y, Nakamura E, Nguyen MT, Suva LJ, Swain FL, Razzaque MS, Mackem S, Lanske B. 2007. Indian Hedgehog produced by postnatal chondrocytes is essential for maintaining a growth plate and trabecular bone. Proc Natl Acad Sci USA 104:6382–6387.

Marfella-Scivittaro C, Quinones A, Orellana SA. 2002. cAMP-dependent protein kinase and proliferation differ in normal and polycystic kidney epithelia. Am J Physiol Cell Physiol 282:C693–C707.

Meldolesi J. 2008. Inhibition of adipogenesis: A new job for the ER Ca²⁺ pool. J Cell Biol 182:11–13.

Nagata A, Tanaka T, Minezawa A, Poyurovsky M, Mayama T, Suzuki S, Hashimoto N, Yoshida T, Suyama K, Miyata A, Hosokawa H, Nakayama T, Tatsuno I. 2009. cAMP activation by PACAP/VIP stimulates IL-6 release and inhibits osteoblastic differentiation through VPAC2 receptor in osteoblastic MC3T3 cells. J Cell Physiol 221:75–83.

Nauli SM, Alenghat FJ, Luo Y, Williams E, Vassilev P, Li X, Elia AE, Lu W, Brown EM, Quinn SJ, Ingber DE, Zhou J. 2003. Polycystins 1 and 2 mediate mechanosensation in the primary cilium of kidney cells. Nat Genet 33:129–137.

Nauli SM, Rossetti S, Kolb RJ, Alenghat FJ, Consugar MB, Harris PC, Ingber DE, Loghman-Adham M, Zhou J. 2006. Loss of polycystin-1 in human cyst-lining epithelia leads to ciliary dysfunction. J Am Soc Nephrol 17:1015–1025.

Neal JW, Clipstone NA. 2002. Calcineurin mediates the calcium-dependent inhibition of adipocyte differentiation in 3T3-L1cells. J Biol Chem 277:49776–49781.

Praetorius HA, Spring KR. 2001. Bending the MDCK cell primary cilium increases intracellular calcium. J Membr Biol 184:71–79.

Praetorius HA, Spring KR. 2003. Removal of the MDCK cell primary cilium abolishes flow sensing. J Membr Biol 191:69–76.

Qian Q, Hunter LW, Li M, Marin-Padilla M, Prakash YS, Somlo S, Harris PC, Torres VE, Sieck GC. 2003. Pkd2 haploinsufficiency alters intracellular calcium regulation in vascular smooth muscle cells. Hum Mol Genet 12: 1875–1880.

Qiu N, Cao L, David V, Quarles LD, Xiao Z. 2010. Kif3a deficiency reverses the skeletal abnormalities in Pkd1 deficient mice by restoring the balance between osteogenesis and adipogenesis. PLoS One 5:e15240.

Saraga-Babic M, Vukojevic K, Bocina I, Drnasin K, Saraga M. 2011. Ciliogenesis in normal human kidney development and post-natal life. Pediatr Nephrol DOI: 10.1007/s00467-011-1941-7.

Shiba D, Takamatsu T, Yokoyama T. 2005. Primary cilia of inv/inv mouse renal epithelial cells sense physiological fluid flow: Bending of primary cilia and Ca2+ influx. Cell Struct Funct 30:93–100.

Starremans PG, Li X, Finnerty PE, Guo L, Takakura A, Neilson EG, Zhou J. 2008. A mouse model for polycystic kidney disease through a somatic in-frame deletion in the 5′ end of Pkd1. Kidney Int 73:1394–1405.

Sun C, Wang L, Yan J, Liu S. 2011. Calcium ameliorates obesity induced by high-fat diet and its potential correlation with p38 MAPK pathway. Mol Biol Rep DOI: 10.1007/s11033-011-0916-x.

Sutters M, Yamaguchi T, Maser RL, Magenheimer BS, St John PL, Abrahamson DR, Grantham JJ, Calvet JP. 2001. Polycystin-1 transforms the cAMP growth-responsive phenotype of M-1cells. Kidney Int 60:484–494.

Szabo E, Qiu Y, Baksh S, Michalak M, Opas M. 2008. Calreticulin inhibits commitment to adipocyte differentiation. J Cell Biol 182:103–116.

Tintut Y, Parhami F, Le V, Karsenty G, Demer LL. 1999. Inhibition of osteoblast-specific transcription factor Cbfa1 by the cAMP pathway in osteoblastic cells. Ubiquitin/proteasome-dependent regulation. J Biol Chem 274:28875–28879.

Tsang KM, Starost MF, Nesterova M, Boikos SA, Watkins T, Almeida MQ, Harran M, Li A, Collins MT, Cheadle C, Mertz EL, Leikin S, Kirschner LS, Robey P, Stratakis CA. 2010. Alternate protein kinase A activity identifies a unique population of stromal cells in adult bone. Proc Natl Acad Sci USA 107:8683–8688.

Tsuang YH, Sun JS, Chen LT, Sun SC, Chen SC. 2006. Direct effects of caffeine on osteoblastic cells metabolism: The possible causal effect of caffeine on the formation of osteoporosis. J Orthop Surg Res 1:7.

Wallace DP. 2011. Cyclic AMP-mediated cyst expansion. Biochim Biophys Acta 1812:1291–1300.

Wang W, Zhang X, Zheng J, Yang J. 2010. High glucose stimulates adipogenic and inhibits osteogenic differentiation in MG-63cells through cAMP/protein kinase A/extracellular signal-regulated kinase pathway. Mol Cell Biochem 338:115–122.

Wilson PD. 2004. Polycystic kidney disease. N Engl J Med 350:151–164.

Xia SL, Ferrier J. 1992. Propagation of a calcium pulse between osteoblastic cells. Biochem Biophys Res Commun 186:1212–1219.

Xiao ZS, Quarles LD. 2010. Role of the polycytin-primary cilia complex in bone development and mechanosensing. Ann N Y Acad Sci 1192:410–421.

Xiao ZS, Hjelmeland AB, Quarles LD. 2004. Selective deficiency of the "bone-related" Runx2-II unexpectedly preserves osteoblast-mediated skeletogenesis. J Biol Chem 279:20307–20313.

Xiao Z, Zhang S, Mahlios J, Zhou G, Magenheimer BS, Guo D, Dallas SL, Maser R, Calvet JP, Bonewald L, Quarles LD. 2006. Cilia-like structures and polycystin-1 in osteoblasts/osteocytes and associated abnormalities in skeletogenesis and Runx2 expression. J Biol Chem 281:30884–30895.

Xiao Z, Zhang S, Magenheimer BS, Luo J, Quarles LD. 2008. Polycystin-1 regulates skeletogenesis through stimulation of the osteoblast-specific transcription factor RUNX2-II. J Biol Chem 283:12624–12634.

Xiao Z, Zhang S, Cao L, Qiu N, David V, Quarles LD. 2010. Conditional disruption of Pkd1 in osteoblasts results in osteopenia due to direct impairment of bone formation. J Biol Chem 285:1177–1187.

Xiao Z, Dallas M, Qiu N, Nicolella D, Cao L, Johnson M, Bonewald L, Quarles LD. 2011. Conditional deletion of Pkd1 in osteocytes disrupts skeletal mechanosensing in mice. FASEB J 25:2418–2432.

Yamaguchi T, Pelling JC, Ramaswamy NT, Eppler JW, Wallace DP, Nagao S, Rome LA, Sullivan LP, Grantham JJ. 2000. cAMP stimulates the in vitro proliferation of renal cyst epithelial cells by activating the extracellular signal-regulated kinase pathway. Kidney Int 57:1460–1471.

Yamaguchi T, Wallace DP, Magenheimer BS, Hempson SJ, Grantham JJ, Calvet JP. 2004. Calcium restriction allows cAMP activation of the B-Raf/ERK pathway, switching cells to a cAMP-dependent growth-stimulated phenotype. J Biol Chem 279:40419–40430.

Yamaguchi T, Hempson SJ, Reif GA, Hedge AM, Wallace DP. 2006. Calcium restores a normal proliferation phenotype in human polycystic kidney disease epithelial cells. J Am Soc Nephrol 17:178–187.

Yang DC, Tsay HJ, Lin SY, Chiou SH, Li MJ, Chang TJ, Hung SC. 2008. cAMP/PKA regulates osteogenesis, adipogenesis and ratio of RANKL/OPG mRNA expression in mesenchymal stem cells by suppressing leptin. PLoS One 3:e1540.

Yoder BK, Mulroy S, Eustace H, Boucher C, Sandford R. 2006. Molecular pathogenesis of autosomal dominant polycystic kidney disease. Expert Rev Mol Med 8:1–22.